*Transport in Porous Media* **3** (1988), 473–489.



# Two-Dimensional Adaptive Eulerian–Lagrangian Method for Mass Transport with Spatial Velocity Distribution

SHAUL SOREK*
*Ben-Gurion University of the Negev, J. Blaustein Institute for Desert Research, The Water Resources Research Center, Sede Boqer Campus 84993, Israel*

(Received: 11 June 1987; revised: 7 June 1988)

**Abstract.** A Eulerian–Lagrangian scheme is used to solve the two-dimensional advection-dispersion equation. Concentration and its partial differential operator are decomposed into advection and dispersion terms. Thus, advection is formally decoupled from dispersion and solved by continuous forward particle tracking. Dispersion is handled by implicit finite elements on a fixed Eulerian grid. Translation of steep gradients of concentration in advection-dominated flow regimes, is done without numerical distortion. Continuous spatial distribution of velocities are evaluated by using Galerkin's approach in conjunction with Darcy's law based on hydraulic input data from each element. The method was implemented on coarse FE grid with linear shape functions, demonstrating no over/under shooting and practically no numerical dispersion. Simulations, covering a wide range of Peclet numbers, yield high agreement with analytic and practical results.

**Key words.** Advection, dispersion, particles, characteristics, finite-element, continuous fluid velocity.

## 1. Nomenclature

| | |
|---|---|
| $b$ | layer thickness |
| $c$ | solute concentration |
| $\bar{c}$ | advection part of concentration |
| $\mathring{c}$ | dispersion part of concentration |
| $c^*$ | source concentration |
| $\mathbf{D}$ | tensor of hydrodynamic dispersion |
| $D_m$ | molecular diffusion |
| $h$ | hydraulic head |
| $N$ | total number of nodes in an element |
| $\mathbf{n}$ | unit vector perpendicular to the boundary, directed outward |
| $P_t$ | total number of particles covering a node |
| $\mathbf{q}$ | Darcy's velocity vector |
| $Q$ | source flux |

* Present address: Department of Bio-Medical Engineering, Technion-Israel Institute of Technology, Haifa 32000, Israel.

$s$ portion of retardation factor
$t$ time
$T_f$ final evolution time
$\mathbf{T}$ transmissivity tensor
$\mathbf{v}$ fluid velocity vector
$\mathbf{x}$ position vector
$x, y$ spatial coordinates

*Symbols*

$\nabla$ gradient vector
$\frac{\partial}{\partial t}$ partial time derivative
$\frac{\mathrm{D}}{\mathrm{D}T}$ hydrodynamic time derivative
$\Delta( )$ difference

*Greek Symbols*

$\alpha_\Gamma$ factor controlling the type of boundary condition
$\alpha_L, \alpha_T$ longitudinal and transverse dispersivities respectively
$\gamma$ fluid's specific weight
$\delta$ Kronecker delta function
$\lambda$ radioactive decay
$\epsilon$ porosity
$\xi$ shape function
$\Sigma$ summation

*Superscripts*

$( )^k$ value at present time level
$( )^{k+1}$ value at front time level
$^k( )$ value for 'single step reverse tracking'
$\hat{}$ finite element approximation
$\cdot$ time derivative

*Subscripts*

$\Gamma$ value along boundary
$p$ value associated with a particle
$n$ value at a node

## 2. Introduction

Most conventional numerical methods for solving the advection-dispersion equation can be classified under two major categories – Eulerian or Lagrangian, depending on whether the transport phenomena are of a parabolic or hyperbolic nature. In the Eulerian category, the governing equation is discretized on a grid

fixed in space, the Lagrangian category utilizes either a deforming grid or a fixed grid in deforming coordinates. A review of these methods can be found in a paper by Neuman (1981). A third approach, the mixed Eulerian–Lagrangian method, combines the simplicity of the fixed grid with the computational power of the Lagrangian approach which is especially effective in regions with high Peclet numbers. To implement this approach, Baptista *et al.* (1986) and Holly *et al.* (1984), solve for advection by shifting particles, while dispersion is solved on a fixed grid. This technique is not rigorously splitting the concentration into terms assigned to solve advection and terms to solve dispersion. Thus, when steep concentration gradients are advected in conjunction with high Peclet numbers, numerical dispersion results, although high-order interpolation schemes are used (Baptista, 1986). The master of these problems is introduced in a novel method that rigorously decomposes the state variable, its partial differential operator, its initial and boundary conditions into advection and dispersion (residual) terms. This method was developed for transport problems (Neuman and Sorek, 1982; Neuman, 1984; Sorek, 1984; Sorek, 1985a; and Sorek, 1987) and for flow problems (Sorek, 1985a; Sorek, 1985b; Sorek and Braester, 1986).

The novel technique consists of two steps, (1) formal decomposition of the state variable field into two parts, one controlled by pure advection, the other essentially by dispersion; and (2) solution of the resulting advection problem by the method of the characteristics for forward particle tracking coupled with an implicit finite element solution of the residual problem on a fixed grid.

Translation of each particle is a function of a fluid velocity regime. The particle's forward position dictates which of the grid nodes will be affected by the particle's load. Hence, spatial continuous velocities are of utmost importance for the solution of the residual problem.

Following Yeh (1981), a procedure will be described to evaluate spatial continuous fluid velocities on the basis of hydraulic information given at each element.

## 3. Theory

Consider the advection-dispersion equation for an effluent constituent in an incompressible flow

$$(1+s)\frac{\partial(\epsilon C)}{\partial t} = \nabla \cdot (\mathbf{D}\nabla C - \epsilon \mathbf{v} C) - \epsilon\lambda C + QC^*, \tag{1}$$

where $(1+s) > 0$ retardation factor (reduction of the apparent velocity due to adsorption or similar phenomena). $\epsilon$ – porosity (ratio of pores volume to the total volume) coefficient; $t$ – time; $C$ – solute concentration; $\nabla$ – gradient operator; $\mathbf{D}$ – tensor of hydrodynamic dispersion (symmetric and semi-positive); $\mathbf{v}$ – fluid velocity vector; $\lambda > 0$ – radioactive decay coefficient; $Q$ – source flux; $C^*$ – concentration associated with the source. (For a detailed study of hydrology terms, see Bear 1979.)

The hydrodynamic dispersion in dimensions $x$ and $y$ can be written as

$$D_{xx} = D_m + \frac{\alpha_L v_x^2 + \alpha_T v_y^2}{|\mathbf{v}|}, \tag{2.1}$$

$$D_{yy} = D_m + \frac{\alpha_L v_y^2 + \alpha_T v_x^2}{|\mathbf{v}|}, \tag{2.2}$$

$$D_{xy} = (\alpha_L - \alpha_T)\frac{v_x v_y}{|\mathbf{v}|}. \tag{2.3}$$

Here $D_m$ is the molecular diffusion; $\alpha_L$, $\alpha_T$ are longitudinal and transverse dispersivities, respectively.

Equation (1) is to be solved for $C$, subject to the initial condition and boundary conditions respectively.

$$C_{(\mathbf{x},0)} = C_{0(\mathbf{x})}, \tag{3}$$

$$(-\epsilon \mathbf{D}\nabla C + \mathbf{q}C)\cdot \mathbf{n} + \alpha_\Gamma(t)\cdot(C - C_\Gamma(t)) = Q_\Gamma(t)\cdot C_\Gamma^*, \tag{4}$$

where $\mathbf{x}$ is the position vector, $\mathbf{q} = \epsilon \mathbf{v}$ – Darcy's velocity vector, $\mathbf{n}$ denotes the unit vector perpendicular to the boundary and directed outward, $C_0$, $C_\Gamma$, $Q_\Gamma$ are prescribed functions and $\alpha_\Gamma$ controls the type of condition prevailing along the boundary.

The Dirichlet condition for prescribing $C$ is

$$C - C_\Gamma = 0; \quad \alpha_\Gamma \to \infty. \tag{5.1}$$

The Cauchy condition for assigning mass flux ($Q_\Gamma C_\Gamma^*$)

$$(-\mathbf{D}\nabla C + \mathbf{q}C)\cdot \mathbf{n} = Q_\Gamma C_\Gamma^*; \quad \alpha_\Gamma = 0, \tag{5.2}$$

otherwise a mixed condition ($0 \leqslant \alpha_\Gamma < \infty$).

Equation (5.2) applies to inflow and no-flow boundaries; along outflow boundaries, the Neuman condition is commonly assumed to be

$$\mathbf{D}\nabla C \cdot \mathbf{n} = 0. \tag{5.3}$$

Let us now write the equation of continuity for the fluid

$$\frac{\partial(\epsilon\gamma)}{\partial t} + \nabla\cdot(\mathbf{q}\gamma) = \gamma Q \tag{6}$$

multiplying Equation (6) by $C$, regarding the incompressibility, reads

$$C\frac{\partial \epsilon}{\partial t} + C\nabla\cdot\mathbf{q} = CQ. \tag{7}$$

In view of Equations (1) and (7), we thus obtain

$$\epsilon\frac{\partial C}{\partial t} + s\frac{\partial(\epsilon C)}{\partial t} = \nabla\cdot(\epsilon\mathbf{D}\nabla C) - \epsilon\mathbf{v}\cdot\nabla C - \epsilon\lambda C + Q(C^* - C). \tag{8}$$

Note that if the solute's concentration equals source concentration, the last term in (8) is omitted.

Using the hydrodynamic derivative

$$\frac{\mathrm{D}}{\mathrm{D}t} = \frac{\partial}{\partial t} + \mathbf{v} \cdot \nabla, \tag{9}$$

Equation (8) is rewritten to

$$\epsilon \frac{\mathrm{D}C}{\mathrm{D}t} + s \frac{\partial(\epsilon C)}{\partial t} = \nabla \cdot (\epsilon \mathbf{D} \nabla C) - \epsilon \lambda C + Q(C^* - C). \tag{10}$$

Here, $C$ no longer represents the concentration at a point in spacetime, but rather that of a fluid particle moving along a characteristic path described by

$$\mathrm{D}\mathbf{x} = \mathbf{v}\, \mathrm{D}t. \tag{11}$$

Let us now decompose the concentration into an advection part $\bar{C}$ and a residual $\mathring{C}$ representing the dispersion part

$$C = \bar{C} + \mathring{C}. \tag{12}$$

One way to perform such a decomposition is to let $\bar{C}$ satisfy

$$\frac{\mathrm{D}\bar{C}}{\mathrm{D}t} = 0, \tag{13}$$

subject to

$$\bar{C}_{(\mathbf{x},0)} = C_{0(\mathbf{x})}, \tag{14}$$

$$\mathbf{q}\bar{C} \cdot \mathbf{n} + \alpha_\Gamma(\bar{C} - C_\Gamma) = Q_\Gamma C_\Gamma^*. \tag{15}$$

The conditions along the outflow boundaries have no effect on $\bar{C}$ and are thus irrelevant. $\bar{C}$ remains constant in time; thus, the 'advection problem' as given by (13)–(15) can be solved within each time step independently of the 'dispersion problem' represented by $\mathring{C}$.

In view of Equations (3)–(4), and (13)–(15), the residual concentration $\mathring{C}$ is governed by

$$\epsilon \frac{\mathrm{D}\mathring{C}}{\mathrm{D}t} + s \frac{\partial(\epsilon C)}{\partial t} = \nabla \cdot (\epsilon \mathbf{D} \nabla C) - \epsilon \lambda C + Q(C^* - C), \tag{16}$$

subject to

$$\mathring{C}_{(\mathbf{x},0)} = 0, \tag{17}$$

$$(-\epsilon \mathbf{D} \nabla C + \mathbf{q}\mathring{C}) \cdot \mathbf{n} + \alpha_\Gamma \mathring{C} = 0. \tag{18}$$

It was demonstrated that the hyperbolic-parabolic advection-dispersion problem defined by (1)–(4) can be formally decoupled into a purely hyperbolic 'advection problem', defined in terms of $\bar{C}$, and a parabolic residual 'dispersion

problem', defined in terms of $\mathring{C}$. The approach is to first solve the advection problem for $\bar{C}$ and then the residual dispersion problem for $\mathring{C}$. Another alternative is to solve (10)–(11) in a Lagrangian form (without resorting to decomposition of $C$) with the aid of the so-called *single-step reverse particle tracking* (explained later). The proposed numerical method utilizes both of these alternatives jointly in an adaptive manner.

## 4. Numerical Implementation

The numerical scheme solves Equations (13)–(15) by continuous forward tracking of particles situated around steep fronts, constant sources, etc. At the beginning of each time step, the field concentration is introduced via the particles and the residual dispersion concentration is set to zero.

$$\bar{C}_{(\mathbf{x},t^k)} = C_{(\mathbf{x},t^k)}, \tag{19}$$

$$\mathring{C}_{(\mathbf{x},t^k)} = 0, \tag{20}$$

where $k$ denotes present time level. At the end of the time step, $\bar{C}$ is kept constant and projected onto fixed nodes for the solution of Equations (16)–(18).

### 4.1. PARTICLE TRACKING TECHNIQUE

Let us define a time step $\Delta t$ as the difference between the front time level $t^{k+1}$ and the present time level $t^k$:

$$\Delta t = t^{k+1} - t^k. \tag{21}$$

Let $\mathbf{x}_p$ be the position vector of particle $p$. Denoting the advective concentration associated with $p$ at time $t^k$ by $\bar{C}_p^k$, then by virtue of (19), we write

$$\bar{C}_p^k \equiv \bar{C}_{(\mathbf{x}_p,t^k)} = C_{(\mathbf{x}_p,t^k)}. \tag{22}$$

For a particle along boundary $\Gamma$ at location $\mathbf{X}_\Gamma$, in view of (15), we obtain

$$\bar{C}_p^k = \frac{\alpha_\Gamma C_\Gamma + Q_\Gamma C_\Gamma^*}{\mathbf{q}\cdot\mathbf{n} + \alpha_\Gamma}\Big|_{\mathbf{x}_\Gamma,t^k}. \tag{23}$$

The concentrations defined by (22)–(23) remain constant over the period $\Delta t$. By virtue of (11), the particle's forward distance $\mathbf{X}_p^{k+1}$ is obtained by

$$\mathbf{X}_p^{k+1} = \mathbf{X}_p^k + \int_{t^k}^{t^{k+1}} \mathbf{v}\,Dt. \tag{24}$$

At the end of this time step, the $\bar{C}$ values are projected onto fixed nodes covered by clouds, using the distance weighting function $\omega_p$ associated with each particle

$$\omega_P = \frac{1/d_p}{\sum_{P_i} 1/d_P}, \tag{25}$$

where $d_p$ is the distance from particle $p$ to a fixed node and $P_t$ is the total number of particles in the clouds covering the latter. The reflected value of $\bar{C}$ upon node $n$ is denoted by $k_{C_n}$. By virtue of (22), we have

$$^kC_n \equiv \bar{C}_{(\mathbf{x}_n, t^{k+1})} = \sum_{P_t} \omega_p \bar{C}_p^k. \tag{26}$$

Thus we associate the nodes with source terms projected from clouds of the particles covering those nodes.

To comply with the hydrodynamic derivative in (16), for nodes covered by clouds (or not covered as in (10)), we use an alternative approach called *single step reverse particle tracking*.

We start by approximating the concentration within each element using its nodal values $C_n$ and a basis interpolation function $\xi_n$. We write

$$C_{(\mathbf{x},t)} \cong \hat{C}_{(\mathbf{x},t)} = \sum_{n=1}^{N} C_n(t)\xi_n(\mathbf{x}), \tag{27}$$

where $N$ is the total number of nodes in the element and $\xi_n$ is an interpolation function described by

$$\xi_n(\mathbf{x}_m) = \delta_{nm} = \begin{cases} 1; & n = m, \\ 0; & n \neq m. \end{cases} \tag{28}$$

Here $\delta_{nm}$ is the Krönecker delta function.

In the single step reverse particle tracking method, we then evaluate $^kC_n$ by moving a fictitious point from a backward position $k_{\mathbf{x}_n}$ so that at the end of the time step it merges with node $n$. Again, in view of (11), we have

$$^k\mathbf{x}_n = \mathbf{x}_n^{k+1} - \int_{t^k}^{t^{k+1}} \mathbf{v}\, Dt. \tag{29}$$

When $\mathbf{v} \neq \mathbf{v}(t)$, Equation (29) yields a constant backward position meaning that a single evaluation of $k_{\mathbf{x}_n}$ suffices. Thus, by virtue of (27) for nodes covered by clouds of particles, we can write

$$^k\mathring{C}_n = \sum_{n=1}^{N} \mathring{C}_n^k \xi_n(^k\mathbf{x}_n). \tag{30.1}$$

For nodes not covered by clouds we rewrite (30.1) to the form

$$^kC_n = \sum_{n=1}^{N} C_n^k \xi_n(^k\mathbf{x}_n). \tag{30.2}$$

This single step reverse formalism is much more efficient computerwise compared with forward particle tracking.

4.2. FIXED GRID TECHNIQUE

Let $A^e$ denote the element area, and application of the Galerkin orthogonalization process to (16) yields,

$$\int_{A^e}\left[\frac{\mathrm{D}\mathring{C}}{\mathrm{D}t}+s\frac{\partial(\epsilon\hat{C})}{\partial t}-\nabla\cdot(\epsilon\mathbf{D}\nabla\hat{C})+\epsilon\lambda\hat{C}-Q(C^*-\hat{C})\right]\xi_n\,\mathrm{d}A^e=0. \tag{31}$$

We now approximate the porosity by an effective value $\bar{\epsilon}$ and a constant time derivative $\dot{\epsilon}$, to read

$$\epsilon\cong\bar{\epsilon}+\dot{\epsilon}t. \tag{32}$$

Partial time derivatives are approximated by backwards differences

$$\frac{\partial C_n}{\partial t}\cong\frac{C_n^{k+1}-C_n^k}{\Delta t}, \tag{33}$$

$$\frac{\mathrm{D}\mathring{C}_n}{\mathrm{D}t}\cong\frac{\mathring{C}_n^{k+1}-{}^k\mathring{C}_n}{\Delta t}=\frac{C_n^{k+1}-(\bar{C}_n^{k+1}+{}^k\mathring{C}_n)}{\Delta t}. \tag{34}$$

Note that the $C_n^k$ and $C_n^{k+1}$ denote the total (advective + dispersive) node concentration evaluated at the $t^k$ and $t^{k+1}$ time levels.

Using Green's first identity, adopting the lumped-mass finite element approach, and by virtue of (17)–(18), (31)–(34), we obtain a global matrix form

$$\left[\boldsymbol{A}+\boldsymbol{B}+\boldsymbol{F}+\frac{1}{\Delta t}(\boldsymbol{W}+\boldsymbol{S})\right]C^{k+1}=\mathbf{Q}+\frac{1}{\Delta t}[\boldsymbol{W}({}^k\mathring{C}+\bar{\mathbf{C}}^{k+1})+\boldsymbol{S}\mathbf{C}^k], \tag{35}$$

where, $\boldsymbol{A}$ is the 'Dispersion Matrix', symmetric and semipositive of order $M$ defined as

$$A_{mn}=\int_R\epsilon\mathbf{D}\nabla\xi_m\cdot\nabla\xi_n\,\mathrm{d}R. \tag{36.1}$$

Here, $R$ is the solution domain for time $t$. $\boldsymbol{B}$ is the 'Boundary Matrix', symmetric of order $M$, given by

$$B_{mn}=\int_\Gamma(\mathbf{q}\cdot\mathbf{n}+\alpha_\Gamma)\xi_m\xi_n\,\mathrm{d}\Gamma;\quad\alpha_\Gamma<\infty. \tag{36.2}$$

Here, $\Gamma$ is the boundary line enclosing $R$. If $m$ and $n$ are on an outflow or noflow boundary, then

$$B_{mn}=0. \tag{36.3}$$

For $\alpha_\Gamma\to\infty$, $C_m$ is known and the $m$ equation is superfluous.

$\boldsymbol{F}$ is a symmetric matrix of order $M$ given by

$$F_{mn}=\int_R(\epsilon\lambda+Q+\dot{\epsilon}s)\xi_m\xi_n\,\mathrm{d}R. \tag{36.4}$$

$\boldsymbol{W}$ is a diagonal 'Capacity Matrix' of order $M$ defined as

$$W_{mn} = \delta_{mn} \int_R \epsilon \xi_m \, dR. \tag{36.5}$$

$\boldsymbol{S}$ is the diagonal 'Retardation Matrix' of order $M$ with terms

$$S_{mn} = \delta_{mn} \int_R \epsilon s \xi_m \, dR. \tag{36.6}$$

$\mathbf{Q}$ is a 'Source Vector' of order $M$ given by

$$Q_m = \psi_m + \int_R QC^* \xi_m \, dR. \tag{36.7}$$

Here

$$\psi_m = -\int_\Gamma (\alpha_\Gamma C_\Gamma + Q_\Gamma C_\Gamma^*) \xi_m \, d\Gamma, \quad \alpha_\Gamma < \infty.$$

If $m$ is on a noflow or outflow boundary, then

$$\psi_m = 0, \tag{36.8}$$

for $\alpha_\Gamma \to \infty$ there is no need for the $M$ term.

Once the nodal concentrations are evaluated, the particle concentration is modified. In view of Equation (27), we obtain

$$C_p^{k+1} = \bar{C}_p^k + \hat{C}_{(\mathbf{x}_p, t^{k+1})} = \bar{C}_p^k + \sum_{n=1}^{N} (C_n^{k+1} - {}^kC_n) \xi_n(\mathbf{x}_p), \tag{37}$$

then $\bar{C}_p^{k+1} = C_p^{k+1}$ is set and the particles are redeployed for the next time step.

It is recommended to cover steep fronts, time dependent sources, etc. with clouds of particles, which are eliminated after the fronts have been flattened through dispersion, retardation or decay. The subsequent procedure is then based on the fixed grid in conjunction with *single-step reverse particle tracking*. The criteria for elimination will be described below.

It was found (Neuman and Sorek, 1982) that for a steep concentration gradient, application of (37) may lead to a situation in which the particle concentration is lower or higher than that of the surrounding element nodes

$$C_P^{k+1} < \min_n C_n^{k+1}, \tag{38.1}$$

$$C_P^{k+1} > \max_n C_n^{k+1}. \tag{38.2}$$

To overcome this discontinuity, Equation (37) is replaced by

$$C_p^{k+1} = \sum_{n=1}^{N} C_n^{k+1} \xi_n(\mathbf{x}_p) \tag{39}$$

which completely eliminates all kinks in (38). Thus, after a few consecutive time steps when (38) is not repeated, ${}^{k}\mathbf{C}$ is defined as

$$ {}^{k}\mathbf{C} = \bar{\mathbf{C}}^{k+1} + {}^{k}\mathring{\mathbf{C}}. \tag{40} $$

Upon substitution of (40) in (35), we obtain a solution scheme obviating the need for forward particle tracking.

### 4.3. VELOCITIES BY FINITE ELEMENTS

The following is a method for evaluating nodal velocities from nodal hydraulic heads, transmissivities and layer thickness given at elements of the grid. Velocities are continuous to the same degree as the supplied nodal hydraulic heads (Yeh, 1981).

In view of Darcy's equation, we write

$$ \mathbf{q} = -\frac{\mathbf{T}}{b}\nabla h, \tag{41} $$

where $\mathbf{T}$ is the transmissivity tensor, $b$ is the layer thickness, and $h$ is the hydraulic head. Let the head values be described by a finite element system

$$ h \cong \hat{h} = \sum_{n=1}^{N} h_n(t)\xi_n(\mathbf{x}). \tag{42} $$

Darcy velocities are then approximated using the same basis function

$$ q_i \cong \hat{q}_i = \sum_{n=1}^{N} q_{in}(t)\xi_n(\mathbf{x}); \quad i = 1, 2. \tag{43} $$

Here $i$ denotes the spatial direction.

Applying Galerkin's method to (41) and in view of (42)–(43), a global set for the solution of nodal velocities is described by

$$ \boldsymbol{E}\mathbf{q}_i = \mathbf{H}_i \tag{44} $$

$\boldsymbol{E}$ is the 'mass matrix' symmetric and of order $M$, given by

$$ E_{mn} = \int_R \xi_m \xi_m \, \mathrm{d}R. \tag{45.1} $$

$\mathbf{H}$ is a 'vector of head gradients' in the $i$ direction and of order $M$, given by

$$ H_{im} = -\left(\frac{h}{b}\right)_n \int_R \xi_m T_{ij} \frac{\partial \xi_n}{\partial x_j} \, \mathrm{d}R. \tag{45.2} $$

Note that the solution of (44)–(45) precedes that of the mass-transport problem. Also, when the flow regime is not steady, the solution of (44) is repeated at each time level with a new set of hydraulic inputs, given at the elements.

## 5. Examples

The first two examples are comparisons with analytical solutions describing a general transport problem. The third is a simulation of a practical problem in metric units with the evaluation of spatially distributed velocities.

Basic interpolation functions were chosen linear. The total number of particles was fairly small. Grid Peclet number $P_i$ was well in excess of 2 and grid Courant numbers $C_i$ was in excess of 1. Both numbers are higher than that recommended in the literature (e.g. Burnett and Frind (1986)) and demonstrate the efficiency of the method in computer resources.

EXAMPLE 1: (Figures 1–4). Following the example given by Varoglu and Finn (1982), we solve Equation (10) with the following boundary conditions

$$C_\Gamma(\mathbf{x}_\Gamma, t) = 0,$$

$$\frac{C_{(\mathbf{x},0)}}{C_0} = \begin{cases} 1 - r/r_0, & 0 \leq r \leq r_0 = 800, \\ 0, & \text{elsewhere.} \end{cases}$$

Also, $\Delta x = \Delta y = 200$; $T_f = 50\,000$; $\Delta t = T_f/10 = 5000$; $D_x = D_y = 2$; $v_x = 0.25$; $v_y = 0$; number of particles: 785.

Note that when dispersions are constant, dispersivities ($\alpha_L$, $\alpha_T$), are meaningless.

The grid Peclet number was

$$P_x = \frac{v_x \Delta x}{D_x} = 25, \qquad P_y = \frac{v_y \Delta y}{D_y} = 0$$

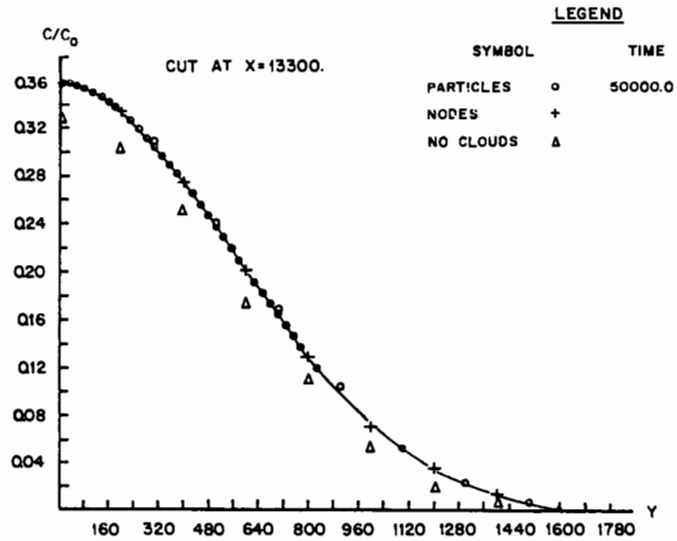


Fig. 1. Values at nodes and particles, and at nodes without clouds.

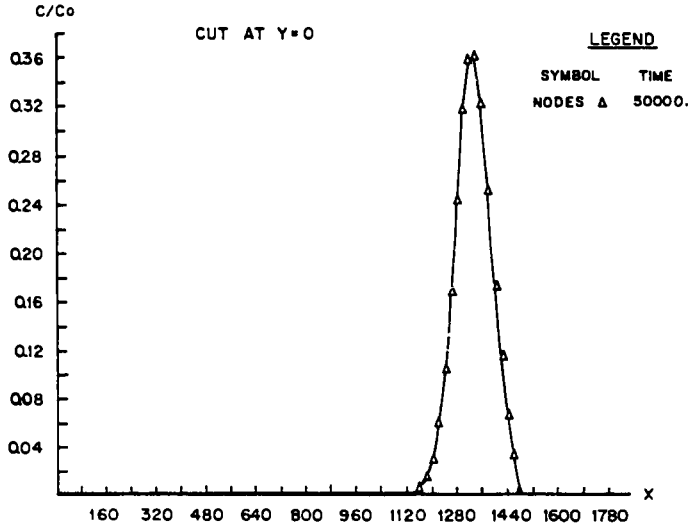


Fig. 2. Values at the nodes.

The grid Courant number was

$$C_x = \frac{v_x \Delta t}{\Delta x} = 6.25, \qquad C_y = \frac{v_y \Delta t}{\Delta y} = 0$$

In Figure 1, the concentration curve of the particles is slightly discontinuous at the border ($y = 800$) where particle distribution changes. This phenomenon is intensified when dealing with steep fronts, but has no effect on the smoothness of

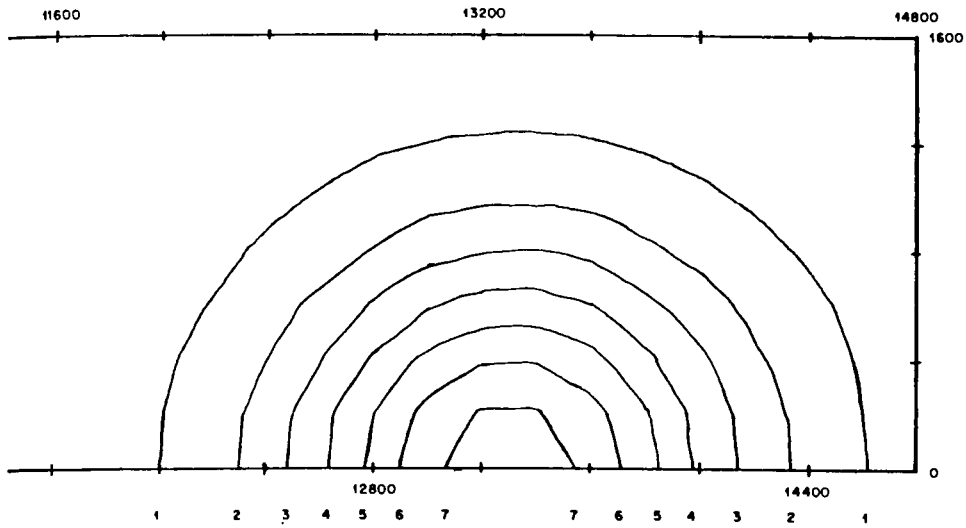


Fig. 3. Contour map from nodal values. Key to contour levels: 1 = 0.03; 2 = 0.08; 3 = 0.13; 4 = 0.18; 5 = 0.23; 6 = 0.28; 7 = 0.33.

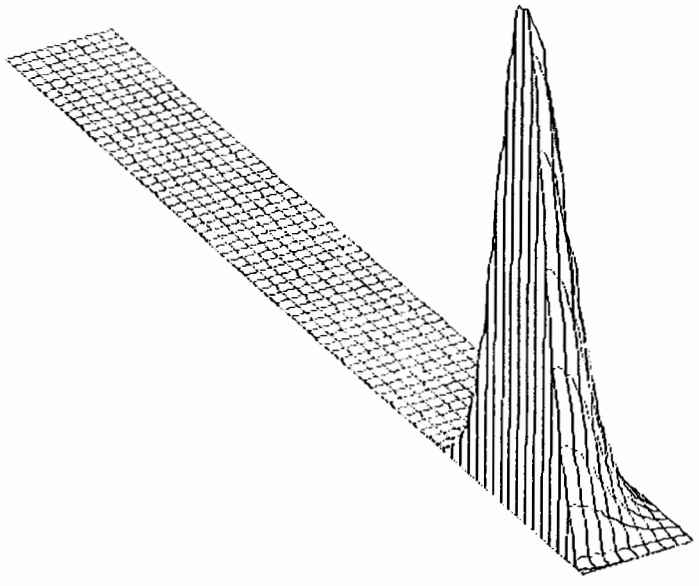

Fig. 4. Perspective view, information from nodes.

the nodal concentration curve. As expected, when particles are not present, the outcome shows numerical dispersion (i.e., smearing of the wave).

EXAMPLE 2: (Figures 5–6). Conditions are the same as in Example 1, except that $D_x = 0$. As expected, the curves of equal concentration (Figure 5), are drawn out in the $y$-direction. As before, changes in particle spatial density within the cloud cause discontinuity of the resulting particle concentration curve (Figure 6). Although a large time increment was used, deviation from the analytical solution is minute.

EXAMPLE 3 (Figures 7–10). In this case, an areal section was simulated with spatially-dependent velocities. Velocity was evaluated from the input of nodal hydraulic heads, transmissivity $T = 1000$ m/day and an effective layer thickness of $b = 0.5$ m. The solution domain was confined by no-flow boundaries except for two open gates through which constant flux was entering and exiting. The initial and boundary conditions for mass transport were

$$C_{(\mathbf{x},0)} = 0; \qquad C_{(x=10\,000\text{ m},t)} = 10\,000;$$

$$C_{(\mathbf{x},0)} = 0 \quad \text{for} \left\{ \begin{array}{c} 1000\text{ m} < x \leq 2000\text{ m} \\ y = 1000\text{ m} \quad \text{and} \quad y = 10\,000\text{ m} \end{array} \right\} \text{location of the gates.}$$

$$\alpha_L = \alpha_T = 500\text{ m}; \qquad s = -1; \qquad \lambda = 0; \qquad \epsilon = 30\%; \qquad \dot{\epsilon} = 0;$$

$$C^* \equiv C; \qquad \Delta x = \Delta y = 1000\text{ m};$$

$$T_f = 1000\text{ days}; \qquad \Delta t = \frac{T_f}{10}; \text{ number of particles: } 185.$$

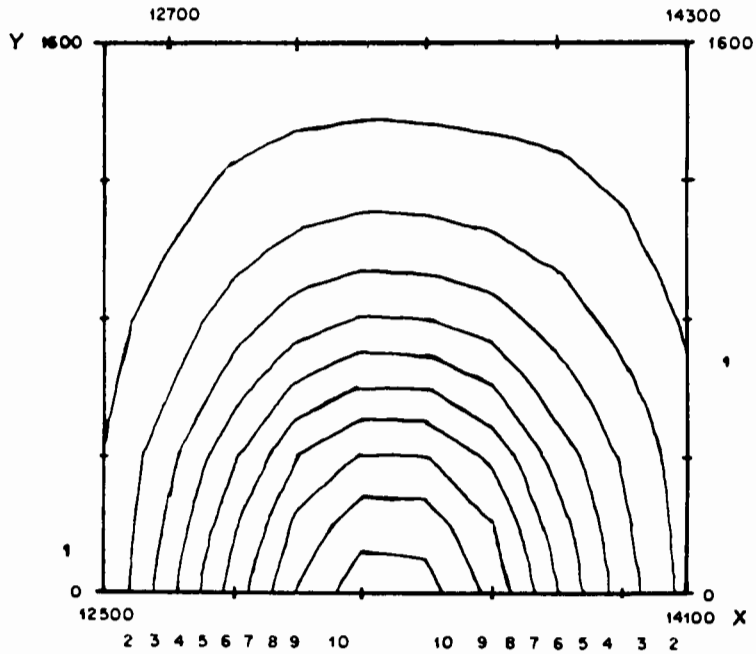


Fig. 5. Contour map from values at particles. Key to contour levels: 1 = 0.03; 2 = 0.08; 3 = 0.13; 4 = 0.18; 5 = 0.23; 6 = 0.28; 7 = 0.33; 8 = 0.38; 9 = 0.43; 10 = 0.48.

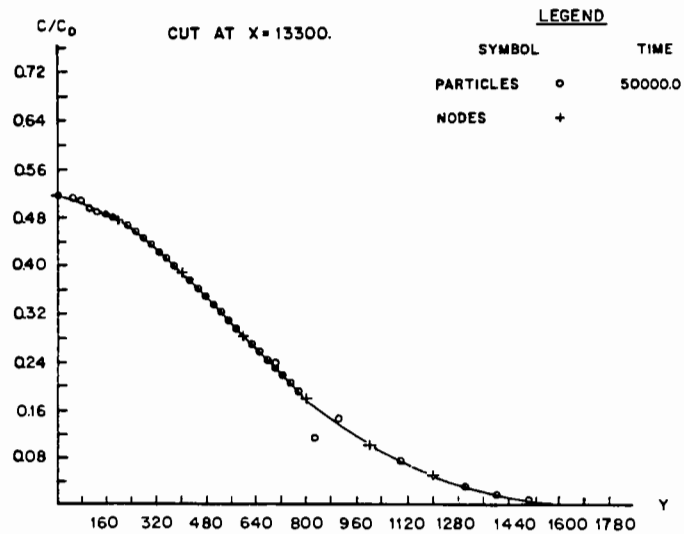


Fig. 6. Values at nodes and at particles.

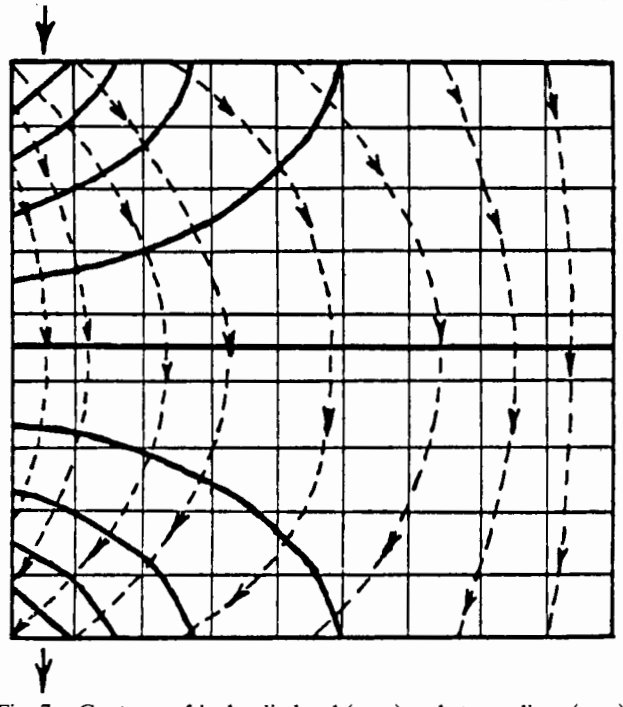

Fig. 7. Contours of hydraulic head (——) and stream lines (----).

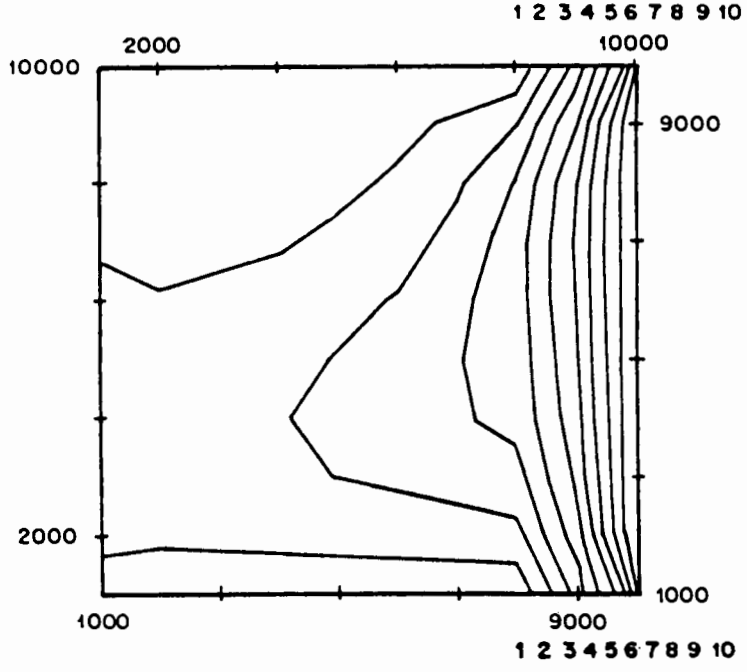


Fig. 8. Contours of concentration after 1000 days. Key to contour levels: 1 = 1000; 2 = 2000; 3 = 3000; 4 = 4000; 5 = 5000; 6 = 6000; 7 = 7000; 8 = 8000, 9 = 9000; 10 = 10 000.

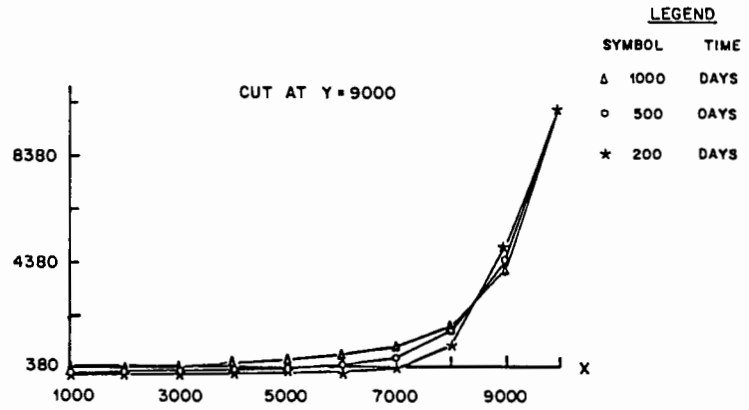


Fig. 9. Evolution curves.

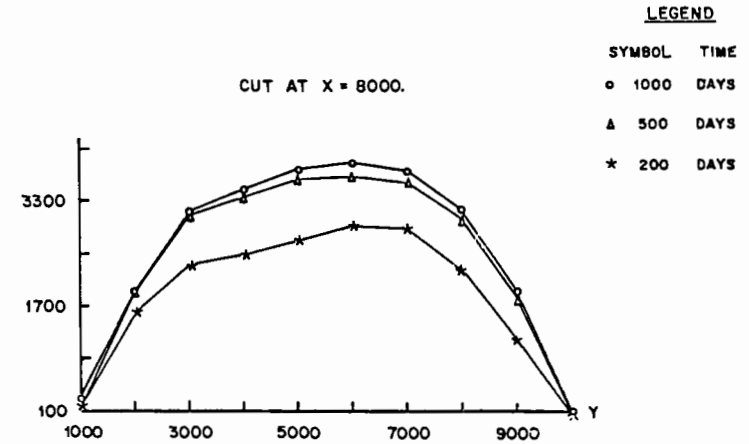


Fig. 10. Evolution curves.

Figure 7 shows the net of equal head lines intersected by stream lines. Figure 8 is the map of concentration contour lines. Figures 9 and 10 are sections through the concentration surface at different time levels.

## 6. Conclusions

(a) The advection-dispersion equation, together with its initial and boundary conditions, can be formally decomposed into pure advection and residual dispersion. The resulting numerical scheme is highly suitable for solving problems incorporating advection dominant phenomena combined with motion of steep fronts. The scheme yields good agreement with analytical solutions and practical simulations by a relatively small numerical effort.

(b) Continuous forward tracking is time consuming, but the program automatically eliminates particles when the front is flattened.
(c) The residual dispersion is solved by finite elements and involves only symmetric and diagonal matrices, thereby reducing the time requirement while improving stability of solutions and computational efficiency.
(d) Courant numbers well in excess of 1 and Peclet numbers that are higher than 2, yield good accuracy.

## References

Baptista, A. M., Adams, E. E., and Stolzenbach, K. D., 1986, Accuracy analysis of the backwards method of characteristics, *Proc. 6th Inter. Conf. F.E.W.R. Lisbon, Portugal*, pp. 477–488.

Bear, J., 1979, *Hydraulics of Groundwater*, McGraw-Hill, New York.

Burnett, R. D. and Frind, E. D., 1986, A comparison of transport simulation in two and three dimensions using alternating direction Galerkin techniques, *Proc. 6th Inter. Conf. F.E.W.R. Lisbon, Portugal*, pp. 459–475.

Varoglu, Ero and Finn, W. D. Laim, 1982, Utilization of the method of characteristics to solve accurately two dimensional transport problems by finite elements, *Inter. J. Num. Methods in Fluids* **2**, 173–184.

Garder, A. O., Peacerman, D. W., and Pozzi, A. L. Jr., 1964, Numerical calculation of multidimensional miscible displacement by the method of characteristics, *Soc. Petrol. Engin. J.* **4**(1), 26–36.

Hinstrup, P., Kej, A., and Kroszynski, U., 1977, A high accuracy two-dimensional transport-dispersion model for environmental applications, *Proc. 18th Intern. Assoc. Hydraul. Res. Congress, Baden-Baden, Germany* **13**, 129–137.

Holly, F. M. and Ussegbo-Polatera, J. M., 1984, Dispersion simulation in two dimensional tidal flow, *J. Hydraulic Eng., ASCE* **110**, 905–926.

Konikow, L. F. and Bredenhoeft, J. D., 1978, *Computer Model of Two-Dimensional Solute Transport and Dispersion in Ground Water*, U.S. Govt. Printing Office, Washington D.C.

Neuman, S. P., 1981, A Eulerian–Lagrangian numerical scheme for the dispersion-convection equation using conjugate space-time grids, *J. Comp. Phys.* **41**(2), 270–294.

Neuman, S. P. and Narasimhan, T. N., 1977, Mixed explicit-implicit iterative finite element scheme for diffusion type problems: I. Theory, *Intern. J. Num. Meth. Engin.* **11**, 309–323.

Neuman, S. P. and Sorek, S., 1982, Eulerian–Lagrangian methods for advection dispersion finite element in water resources, *Proc. 4th Inter. Conf. F.E.W.R. Hanover, Germany*, pp. 1441–1468.

Neuman, S. P., 1984, Adaptive Eulerian–Lagrangian finite element method for advection-dispersion, *Inter. J. Num. Meth. Eng.* **20**, 321–337.

Weddell, D. L. and Sunada, D. K., 1970, Numerical simulation of dispersion in groundwater aquifers, Colorado State Univ. Hydrology Paper 41.

Sorek, S., 1984, ADVDSP two-dimensional adaptive Eulerian–Lagrangian method for the solution of mass-transport equations, *Computer Documentation*, July.

Sorek, S., 1985a, Adaptive Eulerian–Lagrangian method for transport problems in soils, Scientific basis for water resources management, IAHS publ. 153, 393–403.

Sorek, S., 1985b, Eulerian-Lagrangian formulation for flow in soils, theory, *Adv. Water Res.* **8**, 118–120.

Sorek, S. and Braester, C., 1986, An adaptive Eulerian–Lagrangian approach for the numerical simulation of unsaturated flow, *Proc. 6th Inter. Conf. F.E.W.R. Lisbon, Portugal*, pp. 87–100.

Sorek, S., 1988, Eulerian-Lagrangian method for solving transport in aquifers, in press, *Adv. Water Res.*

Yeh, Gour-Tsyh, 1981, On the computation of Darcian velocity and mass balance in the finite element modeling of groundwater flow, *Water Resour. Res.* **17**, 1529–1534.